First-principles study of phase stability of stoichiometric vanadium nitrides

V. I. Ivashchenko, P. E. A. Turchi, V. I. Shevchenko, and E. I. Olifan

Phys. Rev. B **84**, 174108 — Published 14 November 2011

DOI: 10.1103/PhysRevB.84.174108

First-principles study of phase stability of stoichiometric vanadium nitrides

V. I. Ivashchenko,[1] P. E. A. Turchi,[2] V. I. Shevchenko,[1] and E.I. Olifan[1]

[1] *Institute of Problems of Material Science, NAS of Ukraine, Krzhyzhanosky str. 3, 03142 Kyiv, Ukraine*
[2] *Lawrence Livermore National Laboratory (L-352), P.O. Box 808, Livermore, CA 94551, USA*

(ΩDated: October 26, 2011)

First-principles pseudo-potential total-energy and phonon spectrum calculations of various phases of stoichiometric vanadium nitrides with a small number of vanadium and nitrogen vacancies, as well with small carbon and oxygen admixtures were carried out. It was found that the stoichiometric hexagonal and tetragonal vanadium nitrides (VN) were dynamically stable. The NaCl-type VN exhibited lattice instability. The total energy for the computed ground-state phases of VN increased in the sequence: hexagonal (WC-type, $P\bar{6}m2$) – hexagonal (AsNi-type, $P6_3/mmc$) – tetragonal ($P4_2/mcm$) – cubic (NaCl-type, $Fm\bar{3}m$) – cubic (ZnS-type, $F\bar{4}3m$) – cubic (CsCl-type, $Pm\bar{3}m$). At low temperatures, the vacancies in both sublattices stabilize the triclinic phases of V_xN_x, for $x < 0.94$, which is consistent with tetragonal symmetry. At high temperatures, the stability of the NaCl- and WC-type VN structures was estimated using an approach based on band energy smearing. The results obtained indicate that the cubic structure of VN with the fully occupied sublattices will be stable only at high temperatures. The small carbon and oxygen admixtures do not stabilize the cubic phase compared to the hexagonal one. The phase stability of the cubic and hexagonal structures of V_xN_x was explained on the basis of the peculiarities of their electronic densities of states near the Fermi level. The predicted structural transformations in stoichiometric vanadium nitrides are compatible with those observed in experimentally.

PACS numbers: 64.60.Ej, 63.20.dk, 71.15.Nc, 71.20.-b

I. INTRODUCTION

Vanadium nitrides are of interest because of their unique combinations of physical properties that make them important components in hard coatings and optoelectronic devices[1]. Vanadium nitrides crystallize with a NaCl ($B1$)-type structure (space group $Fm\bar{3}m$) at high nitrogen concentration (VN_x, $0.7 \leq x \leq 1.0$)[1,2]. It was reported that, in the nitrogen-rich compounds, vanadium vacancies could also be formed[1]. The most interesting peculiarity of VN_x, for $0.98 \leq x \leq 1.0$, is the cubic-to-tetragonal structural transformation at 205 K (space group $P\bar{4}2m$)[3]. At 20 K, the tetragonal lattice of VN undergoes triclinic distortion[4]. Phonon anomalies were observed in substoichiometric NaCl-type VN_x ($x < 1.0$) at the X point of the Brillouin zone (BZ) by inelastic neutron diffraction measurements[5]. Below, "stoichiometric" will refer to equiatomic composition.

Electronic structure properties and lattice dynamics of vanadium nitrides and related compounds have been reviewed in Refs. 3, 6–9. Therefore, here, we only recall the main studies that pertain directly to the topic of this work. The phonon spectrum calculations of VN revealed that this compound is dynamically instable[6,7]. It was shown that the cubic-to-tetragonal structural transformation in VN is related to the elastic instability that arises due to a coupling between the soft X_3 acoustic mode and spontaneous volume and tetragonal strains[7]. The tetragonal phase with the space group $P\bar{4}2m$ was found to transform into another tetragonal phase with the space group $P4_2/mcm$ (t-VN) when the band energy smearing associated with temperature decreases[7]. The ground-state and phase stability properties of the cubic and hexagonal phases of VN_x have been investigated based on total-energy calculations with a first-principles pseudo-potential method[8,9]. The stoichiometric vanadium nitride was found to have enhanced stability in the WC-type lattice as compared to the experimental NaCl-type structure. Also, it was shown that nitrogen vacancies stabilize the NaCl phase of VN_x compared to WC phases[9]. The stabilization of the NaCl-type over WC-type transition metal compounds with non-metal vacancies was also established on the basis of an analysis of their electronic structures[10,11].

This brief review indicates the contradiction between experiment and theory for stoichiometric vanadium nitride. In particular, according to the first-principles calculations[8,9], the most stable structure of VN is a hexagonal structure, whereas only cubic, tetragonal, and triclinic phases were detected in experiments[1,2,4]. Therefore, the aim of the present investigation is to account for the structural stability of the experimental phases of stoichiometric vanadium nitride in the framework of a first-principles approach. For this purpose, the total energy and phonon spectrum calculations were carried out for several stoichiometric compounds with fully or partially occupied vanadium and nitrogen sublattices, as well as with small carbon and oxygen admixtures in the nitrogen sublattice. The stability of the computed structures is explained based on the peculiarities of their densities of states near the Fermi energy.

The paper is organized as follows. In Sec. II we present our theoretical framework and the computational details. Sec. III contains the results of our calculations together with comments. Finally, Sec. IV contains the main conclusions.

II. DETAILS OF THE FIRST-PRINCIPLES CALCULATIONS

A first-principles pseudo-potential procedure was employed to investigate the cubic, tetragonal, hexagonal and triclinic structures of V_xN_x, for $0.875 \leq x \leq 1.0$. Scalar-relativistic band-structure calculations within the density functional theory (DFT) were carried out for the 2-atom (NaCl($B1$)-, WC-, ZnS-, CsCl-type), 4-atom (AsNi-type), 8-atom (t-VN) unit cells of VN, as well the 64-, 62-, 60- and 58-atom cubic, triclinic supercells originated from the NaCl- and WC-type structures of V_xN_x, $x = 1.0$, 0.96875, 0.9375, 0.90625, 0.875 ($V_{32}N_{32}$, $V_{31}N_{31}$, $V_{30}N_{30}$, $V_{29}N_{29}$, $V_{28}N_{28}$). The initial 64-atom (2×2×2) supercell of NaCl-type VN was constructed from the basic 8-atom cubic cells. The initial 64-atom supercell of WC-type VN was represented with the (4×4×2) supercells constructed on the basis of the 2-atom hexagonal cells. The vacancies in both sublattices were produced by randomly removing the corresponding atoms, making sure that the number of adjacent vacant sites is minimized. Carbon or oxygen atoms were introduced into the initial supercells in the same manner, except that a vacant cite was now occupied with either a carbon or an oxygen atom. The crystalline type, symmetry and number of the atoms in the unit cells of the various structures of stoichiometric vanadium nitrides with a small number of vanadium and nitrogen vacancies (V_xN_x) are summarized in Table I. Below we will denote the structures obtained after atomic relaxation of the initial NaCl- and WC-type supercells as the NaCl-based and WC-based structures, respectively.

The "Quantum-ESPRESSO" first-principles code[12] was used to perform pseudo-potential calculations with Vanderbilt ultra-soft pseudo-potentials to describe the electron-ion interaction[13]. In the Vanderbilt approach[13], the orbitals are allowed to be as soft as possible in the core region so that their plane-wave expansion converges rapidly. For vanadium, the semicore states were treated as valence states. Plane waves up to a kinetic energy cutoff of 38 Ry were included in the basis set. The exchange-correlation potential was treated in the framework of the generalized gradient approximation (GGA) of Perdew-Burke-Ernzerhof (PBE)[14]. Brillouin-zone integrations for the 2-, 4-, 8-, and 58-64-atom cells have been performed using sets of special points corresponding to the (12 12 12), (8 8 8), (4 4 4) and (2 2 2) Monkhorst-Park meshes[15], respectively. For the large supercells, we considered the (2 2 2) mesh that, although it generates a minimum number of k-points, provides an acceptable accuracy. We calculated the E_T values of V_xN_x by using the finer meshes (4 4 4) for NaCl-based and (3 3 6) for WC-based structures, and found the rather well convergence on k-points. As will be shown below, small errors do not impact our conclusions on phase stability (cf. Fig. 4). Also, to verify the effect of atomic configuration on the total energy we carried out total energy calculations for the WC- based and NaCl-based V_7N_7 cells (derived from the V_8N_8 cells) that have the same vacancy concentration, $1 - x = 0.125$, as the large-scale structures $V_{28}N_{28}$. The difference in E_T between the small- and large-scale WC-based and NaCl-based structures is 10.6 meV/atom and 2.6 meV/atom, respectively. These small deviations (cf. Fig. 4) indicate that a change in vacancy configuration weakly influences the total energy. Each eigenvalue was convoluted with a gaussian with width $\sigma = 0.02$ Ry (0.272 eV). Additional calculations were performed using the Fermi-Dirac function for band energy smearing with the parameter $\sigma = 0.02 - 0.05$ Ry (0.272-0.68 eV). All structures were optimized by simultaneously relaxing the atomic basis vectors and the atomic positions inside the unit cells using the Broyden-Fletcher-Goldfarb-Shanno (BFGS) algorithm[16]. The relaxation of the atomic coordinates and of the unit cell was considered to be complete when the atomic forces were less than 1.0 mRy/Bohr (25.7 meV/Å), the stresses were smaller than 0.025 GPa, and the total energy during the structural optimization iterative process was varying by less than 0.1 mRy (1.36 meV). The electronic densities of states (DOS) were calculated using the (12 12 12) mesh for the 64-atom supercells and the (6 6 6) mesh for the 56-, 58-, 60- and 62- atom supercells.

We carried out the spin-polarized total energy calculations for the cubic, tetragonal and hexagonal phases. It was found that these structures relaxed to the corresponding structures computed with neglecting spin polarization.

The above-described pseudo-potential procedure was used to study the phonon spectra of cubic, hexagonal and tetragonal VN in the framework of the density-functional perturbation theory (DFPT) described in Refs. 12 and 17. The first-principles DFPT calculations were carried out for the (6 6 6) q-mesh, and then the phonon densities of states (PHDOS) were computed using the (12 12 12) q-mesh by interpolating the computed phonon dispersion curves. Both the DOS and PHDOS were calculated with the tetrahedron method implemented in the "Quantum-ESPRESSO" code[12]. The partial DOS (PDOS) of the stoichiometric vanadium nitrides were calculated by means of smearing eigenvalues with the gaussian[12].

III. RESULTS AND DISCUSSION

Fig. 1 shows the total energies of VN in various structures as functions of cell volume. The structural parameters of the various phases of stoichimetric vanadium nitrides are summarized in Table I. The total energy (E_T) (in meV/atom) for the computed ground-state phases increases in the sequence: 0.0 (WC-type), 100.9 (AsNi-type), 162.5 (t-VN), 180.9 (NaCl-type), 310.9 (ZnS-type), 681.0 (CsCl-type). Such a sequence indicates that VN has enhanced stability in the WC, AsNi and t-VN structures as compared to the NaCl-type structure. For the sake of comparison, one notes that our

TABLE I. Cell parameters and symmetry of stoichiometric vanadium nitrides with various structures. Notations N_a – number of atoms in the cell; a, b, c – modules of the basis vectors; α, β, γ – angles between the basis vectors. The experimental lattice parameter for $B1$-VN is 4.133 Å[4].

Structure	Symmetry	N_a	a (Å)	b (Å)	c (Å)	α (Degree)	β (Degree)	γ (Degree)
NaCl($B1$)	$Fm\bar{3}m$	2	4.126	4.126	4.126	90	90	90
t-VN	$P4_2/mcm$	8	4.153	4.153	4.046	90	90	90
AsNi	$P6_3/mmc$	4	2.771	2.771	5.149	90	90	120
WC	$P\bar{6}m2$	2	2.751	2.751	2.641	90	90	120
ZnS	$F\bar{4}3m$	2	4.285	4.285	4.285	90	90	90
CsCl	$Pm\bar{3}m$	2	2.539	2.539	2.539	90	90	90
$B1$-$V_{31}N_{31}$	$P1$	62	8.220	8.173	8.173	90.002	90.004	90.001
$B1$-$V_{30}N_{30}$	$P1$	60	8.152	8.150	8.153	90.397	90.407	90.396
$B1$-$V_{29}N_{29}$	$P1$	58	8.132	8.133	8.116	90.034	89.994	90.158
$B1$-$V_{28}N_{28}$	$P1$	56	8.100	8.075	8.101	90.071	90.080	90.060
WC-$V_{31}N_{31}$	$P1$	62	10.954	10.955	5.272	90.008	90.084	120.012
WC-$V_{30}N_{30}$	$P1$	60	10.932	10.977	5.252	89.709	90.086	120.091
WC-$V_{29}N_{29}$	$P1$	58	10.963	10.929	5.240	89.197	90.477	120.129
WC-$V_{28}N_{28}$	$P1$	56	10.945	10.921	5.230	89.060	90.391	120.071

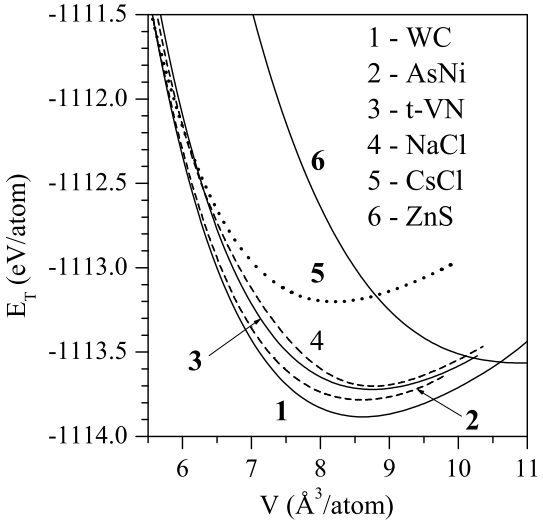

FIG. 1. Total energies (E_T) as functions of cell volume (V) for various phases of VN.

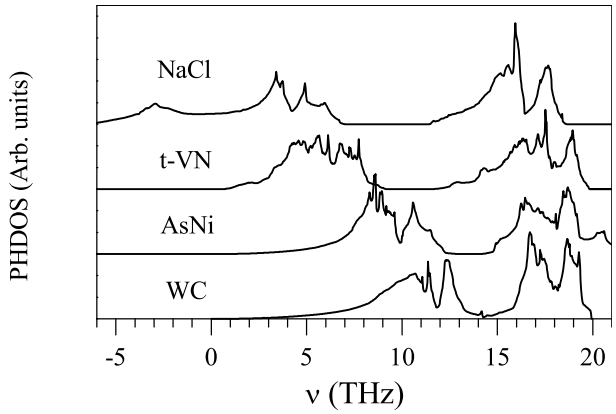

FIG. 2. Phonon densities of states (PHDOS) for the cubic (NaCl), tetragonal (t-VN) and hexagonal (AsNi, WC) structures of VN. The negative frequencies refer to imaginary frequencies.

total energy results are very close to those obtained in Ref. 9 for the AsNi- and NaCl-type structures: 101.0 and 181.7 meV/atom, respectively. Based on these results, one can deduce that only WC-type VN can exist at temperatures close to 0 K. We should recall that the triclinic, tetragonal, and cubic structures of VN are experimentally observed at low (< 20 K), moderate (< 205 K) and high temperatures (> 205 K), respectively[4]. One way to explain this contradiction is to analyze the phonon spectra of the computed structures in their ground state. The motivation is that a given structure cannot be stabilized if its phonon spectrum has imaginary branches that would indicate lattice instability. In Fig. 2 we show the phonon density of states of the four VN structures with the lowest total energies. We preferred to analyze the phonon density of states instead of the phonon dispersion curves along symmetry directions of the Brillouin zone (BZ) to allow for possible soft phonon modes at low-symmetry points of BZ. It follows from Fig. 2 that the acoustic branch shifts towards high frequencies in the sequence NaCl – t-VN – AsNi – WC, which means that the rigidity of the lattice increases in this sequence. What the acoustic frequencies in t-VN are lower compared to those in the hexagonal phases indicates that soft acoustic modes are still present in the phonon spectrum of the tetragonal structure. In contrast to the acoustic branch,

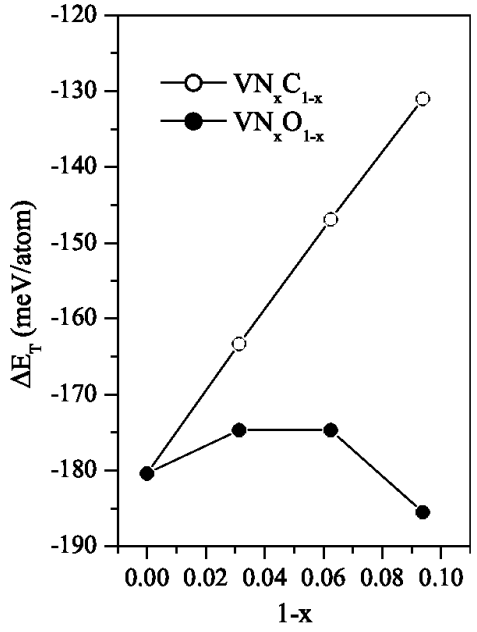

FIG. 3. Differences between the total energies of the WC- and NaCl-based structures of VN_xC_{1-x} and VN_xO_{1-x} ($\Delta E_T = E_T(\mathrm{WC}) - E_T(\mathrm{NaCl})$) as functions of carbon and oxygen concentrations $(1-x)$.

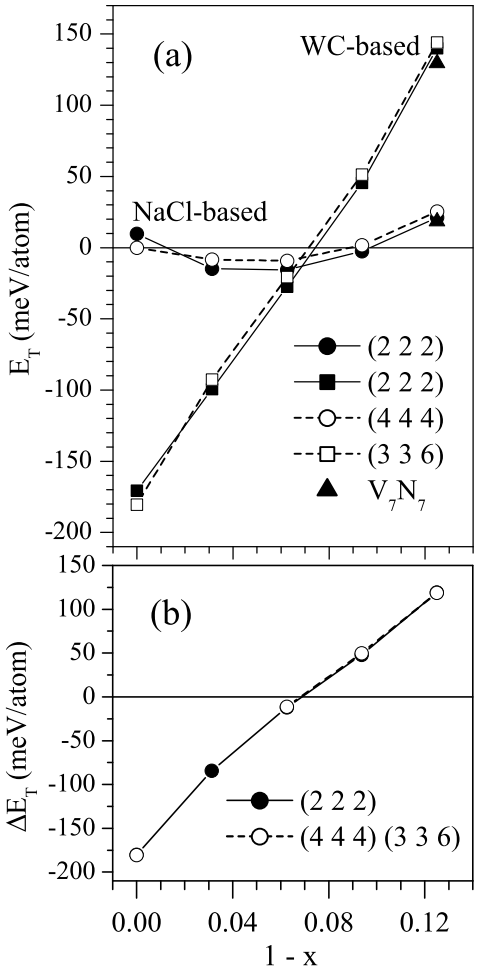

FIG. 4. Total energies of the NaCl- and WC-based structures of V_xN_x (E_T) (a) and the difference $\Delta E_T = E_T(\mathrm{WC}) - E_T(\mathrm{NaCl})$ (b) as functions of the concentration of vanadium and nitrogen vacancies $(1-x)$. The calculations were carried out using different k-point meshes. The total energy E_T of the equilibrium NaCl-based $V_{1.0}N_{1.0}$ ($V_{32}N_{32}$) (with the (4 4 4) mesh) is considered as the reference energy.

the optical phonons in this sequence change very little. We also note that our suggestion about the lattice instability of the hexagonal phases is not confirmed – the hexagonal and tetragonal structures of VN do not show any phonon modes with imaginary frequencies. Instead, it was revealed that NaCl-type VN could not be stabilized because of phonon states with imaginary frequencies (cf. Fig. 2). It should be noted that the present data on phonon spectra are consistent with those obtained for the hexagonal and cubic structures of NbN[18].

Assuming that the small additions of oxygen or carbon could stabilize cubic VN, we have carried out total energy calculations by using the 64-atom NaCl and WC supercells in which nitrogen atoms were substituted by oxygen or carbon atoms. The differences between the total energies (ΔE_T) of the WC- and NaCl-based VN_xC_{1-x} and VN_xO_{1-x}, for $x > 0.9$, are presented in Fig. 3 as functions of carbon and oxygen concentration, $1-x$, respectively. One can see that the small carbon and oxygen admixtures do not stabilize NaCl-VN compared to WC-VN, although the carbon admixture causes a reduction of ΔE_T. The linear extrapolation of the $\Delta E_T(1-x)$ dependencies for VN_xC_{1-x} shows that the carbon will be able to stabilize the cubic-based structure at higher carbon content $1-x > 0.34$. The possible mechanism that leads to phase stability by adding carbon or oxygen atoms will be considered below.

Another structural element that could cause the stabilization of the cubic-like structure of stoichiometric vanadium nitride is a structural vacancy. It is the influence of vanadium and nitrogen vacancies on the structural stability of NaCl- and WC-based V_xN_x that is the subject of our next study. In Fig. 4 we show the total energies of the NaCl- and WC-based structures of V_xN_x as functions of the concentration of vanadium and nitrogen vacancies, $1-x$. The difference between the total energies of both structures decreases as $1-x$ increases. For the vacancy concentration $1-x > 0.06$, the NaCl-based structure is more stable than the WC-based one. The NaCl- and WC-based structures of V_xN_x, for $x < 1.0$ have triclinic symmetry with the space group $P1$. However, a comprehensive analysis of the structural parameters, summarized in Table I, shows that the NaCl-based structure has a triclinic lattice that is consistent with tetragonal symmetry ($a \approx b \neq c$; $\alpha \approx \beta \approx \gamma \approx 90°$) in agreement with experiment[4]. The triclinic structure of WC-based V_xN_x is consistent with hexagonal symmetry ($a \approx b \neq c$; $\alpha \approx \beta \approx 90°$, $\gamma \approx 120°$) (cf. Table I).

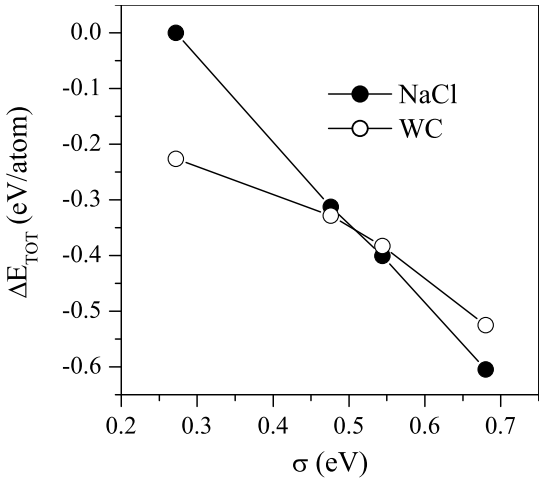

FIG. 5. Total energies of the NaCl- and WC-type VN structures (ΔE_T) as functions of the band energy smearing (σ). The total energy of NaCl-type VN is taken as zero of energy.

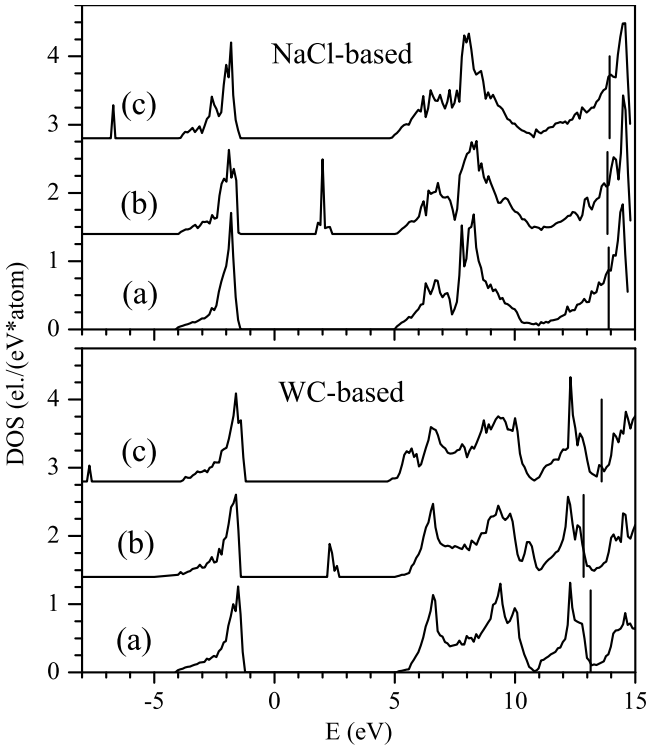

FIG. 6. Densities of states (DOS) of the NaCl- and WC-based structures of $V_{32}N_{32}$ (a), $V_{32}N_{29}C_3$ (b) and $V_{32}N_{29}O_3$ (c). Each vertical line locates the Fermi level.

Since in band energy calculations band energy smearing, σ, is a rather arbitrary parameter one should analyze the influence of band energy smearing on phase stability before we discuss a possible origin of the stabilization of NaCl-type VN. It was clearly pointed out in a recent study that strongly influences the total energy[7]. Our experience shows that the total energy decreases with increasing σ, and the most noticeable change in E_T caused by σ is observed for a structure with a high DOS at the Fermi level, $N(E_F)$. Because $N(E_F)$ is significantly higher in NaCl-based VN than in WC-based VN (see below) one expects that a large σ correlates with stabilization of the NaCl-structure relative to the WC-structure. Indeed, the total energy results for NaCl- and WC-type VN for various smearing parameters σ, presented in Fig. 5, show that the hexagonal-to-cubic transition takes place above $\sigma = 0.5$ eV. It is well known that, to a first approximation, the effects of temperature and vacancies result in a smearing of band energies, therefore we can assign the parameter σ to these effects. It should be noted here that our investigation on phase stability of VN has a semi-quantitative character since we correlate in a phenomenological way the smearing parameter σ to temperature and vacancy concentration: "an increase in σ implies a corresponding increase in temperature or vacancy concentration". Nevertheless, such an approach enables us to rather correctly describe the main features of the cubic-to-tetragonal phase transition in vanadium nitride[7]. An increase in σ, which corresponds to an increase in temperature and/or concentration of vacancies, leads to the disappearance of the phonon anomalies and the stabilization of NaCl-based VN[7]. Given these and previous results, we arrive at the following conclusions: i) at high temperatures, only the cubic phase of stoichiometric vanadium nitride will exist; ii) at low temperatures, the triclinic stoichiometric structure of V_xN_x, $x < 0.94$, that is consistent with tetragonal symmetry, will be most stable; iii) in V_xN_x, the minimum concentration of vacancies that causes the stabilization of the cubic-based structure over the hexagonal-based one will decrease with increasing temperature.

To gain more insight into the origin of the changes in electronic structure and stability of both the NaCl- and WC-based structures caused by admixtures, let us analyze the DOS of these structures that contain small carbon or oxygen admixtures. In Fig. 6 we show the electronic spectra of both structures of VN_xC_{1-x} and VN_xO_{1-x}. The partial densities of states of the stoichiometric cubic and hexagonal vanadium nitrides are shown in Fig. 7. It is seen that the electronic spectra of the NaCl- and WC-based structures of $V_{1.0}N_{1.0}$ exhibit three main bands. An analysis of the partial DOSs shows that the low-energy band originates from the N $2s$ state. The next $d-p$ band located around -7 eV is mostly associated with the V d and N p states. The $d-p$ band splits into two sub-bands related to the (V d – N p)σ and (V d – N p)π bonds. This splitting is more noticeable for WC-type structure. Because of the structural peculiarities of the hexagonal phase, the (V d – N p)σ bonds are directed mainly along the c-axis, and the (V d – N p)π bonds are distributed mainly in the plane that is perpendicular to the c-axis. The band related to the (V d – N p)σ bonds are shown in the DOS in the low energy region. Finally, the high-energy metallic d-band is located below and above the Fermi level. Because of the

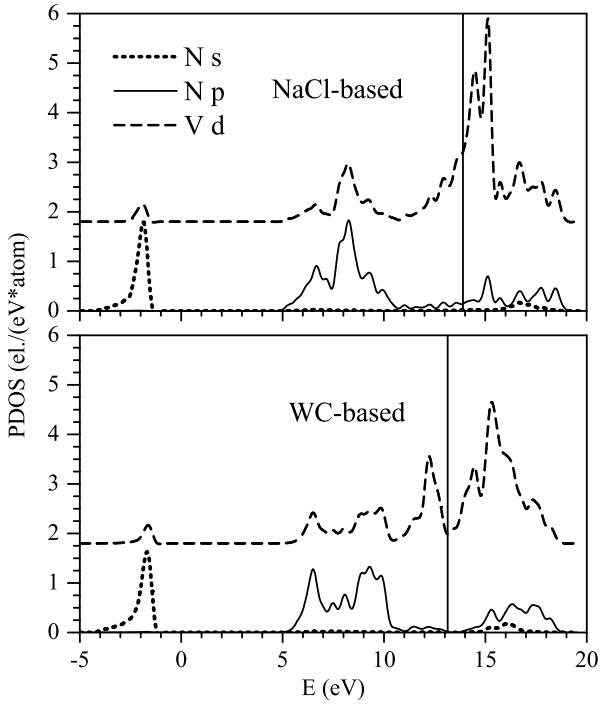

FIG. 7. V d and N s,p partial (local) densities of states (PDOS) of the NaCl- and WC-based structures of $V_{32}N_{32}$. Each vertical line locates the Fermi level.

strong V d – N p interaction, this band splits into a low-energy V d_ε sub-band and a high-energy V d_γ sub-band. In the case of NaCl- type VN, the Fermi level is located below the DOS minimum that separates these sub-bands, whereas in WC-type VN, E_F is located right in this local minimum of the DOS. The calculated PDOSs of VN are consistent with those of stoichiometric transition metal nitrides[19,20].

The substitution of nitrogen by carbon leads to an appearance of additional carbon states below the Fermi level (E_F). On the other hand, the DOS just below E_F changes insignificantly. Therefore, a lowering of EF, caused by a reduction in the valance electron concentration (VEC), leads to a decrease (an increase) of the DOS at E_F, $N(E_F)$, for the NaCl-based (WC-based) structure, as shown in Fig. 6. On the contrary, for VN_xO_{1-x}, an increase in VEC results in the opposite picture: in the NaCl-based structure, $N(E_F)$ increases and, in the WC-based structure, it first slightly decreases and then increase with decreasing x. A comparison of these findings with the total energy trends presented in Fig. 3 clearly indicates the correlation between $N(E_F)$ and phase stability: the lower $N(E_F)$ is, the lower the total energy is.

A different bonding picture is observed for stoichiometric phases of V_xN_x, for $x \leq 1.0$. The DOSs of the NaCl-based and WC-based structures of V_xN_x are shown in

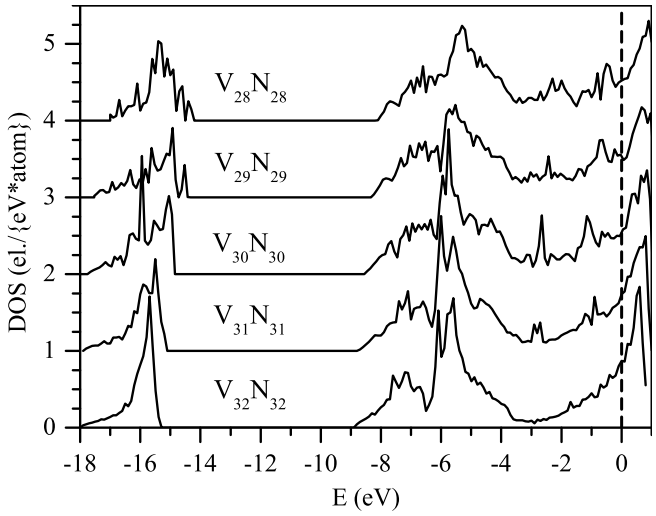

FIG. 8. Density of states (DOS) of NaCl-based V_xN_x. The vertical line locates the Fermi level.

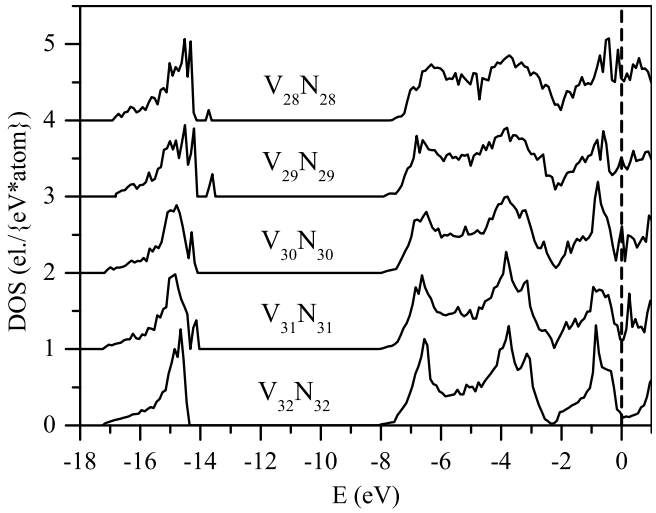

FIG. 9. Density of states (DOS) of WC-based V_xN_x. The vertical line locates the Fermi level.

Figs. 8 and 9. In both structures, vanadium vacancies give rise to additional peaks in the high-energy region of the s- and p-d bands. Based on an analysis of the local DOS, we deduce that these peaks can be assigned to non-bonding nitrogen states. Since these vacancy-induced states are located below E_F, vanadium vacancies shift the Fermi level towards low (high) DOS in the NaCl-(WC-based) structures. It is well known that, in transition metal compounds, "vacancy states", induced with nitrogen vacancies, are localized at the bottom of the metal d-band, and originate from the V-V bonds passing through a nitrogen vacancy[3,18,19]. Fig. 8 shows that, in the DOS of the NaCl- based structures, nitrogen vacancies cause the formation of additional states below the Fermi level and of a local minimum around E_F. As a results, an increase in the number of nitrogen vacancies

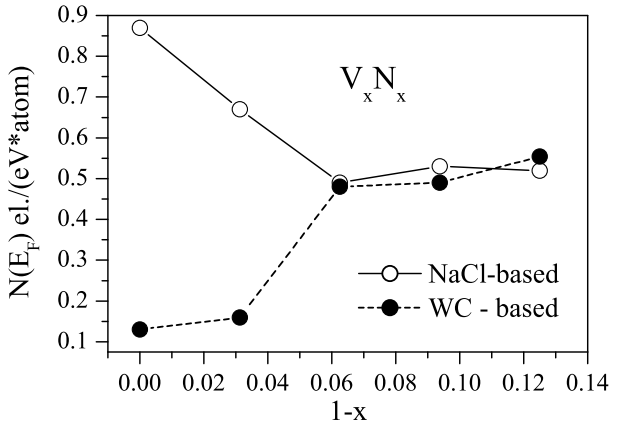

FIG. 10. Density of states at the Fermi level ($N(E_F)$) for the NaCl- and WC-based structures of V_xN_x as functions of the concentration of vanadium and nitrogen vacancies ($1-x$).

leads to a decrease in $N(E_F)$. On the contrary, for the WC-based structure, nitrogen vacancies generate additional states just at E_F, for which case $N(E_F)$ increases with an increase in the number of nitrogen vacancies (cf. Fig. 9).

The behavior just discussed of the DOS at the Fermi level in V_xN_x is illustrated in Fig. 10, where $N(E_F)$ of both the NaCl- and WC-based structures are presented as functions of the vacancy concentrations $1-x$. Based on the results presented in Figs. 4 and 10, we again draw a parallel between $N(E_F)$ and phase stability in V_xN_x: a decrease in x leads to an increase in the DOS at the Fermi level in the WC-based phase and to a decrease in the DOS around E_F in the NaCl-based structure, thereby stabilizing the cubic structure.

Finally, let us analyze the experimental and theoretical data on phase stability for the different structures of vanadium nitrides with small concentrations of vacancies in both the vanadium and nitrogen sublattices. According to recent first-principles studies[9], despite the stabilization of the cubic phases with nitrogen vacancies, only the WC-based VN_x structures, for $x>0.8$, is found to be the most stable. However, experiments clearly indicate that, at low and high temperatures, VN_x crystallize with the NaCl-based structures[1,2,4]. Given these facts and the results of the present investigation, we expect to find NaCl-based structures of VN_x, for small $1-x$, stabilized at low temperatures as long as the substoichiometric vanadium nitrides contain, along with nitrogen vacancies, a small number of vacancies in the vanadium sublattice.

IV. CONCLUSIONS

First-principles pseudo-potential total-energy and phonon spectrum calculations were carried out for stoichiometric vanadium nitrides with a small number of vanadium and nitrogen vacancies and low concentrations of carbon and oxygen admixtures. It was found that the stoichiometric hexagonal and tetragonal vanadium nitrides (VN) were dynamically stable, whereas the NaCl-type VN showed lattice instability. The total energy for the computed ground-state phases of VN increased in the sequence: hexagonal (WC-type, $P\bar{6}m2$) – hexagonal (AsNi-type, $P6_3/mmc$) – tetragonal ($P4_2/mcm$) – cubic (NaCl-type, $Fm\bar{3}m$) – cubic (ZnS-type, $F\bar{4}3m$) – cubic (CsCl-type, $Pm\bar{3}m$). At low temperatures, the vacancies in both sublattices stabilize the triclinic phases of V_xN_x, for $x<0.94$, which is consistent with tetragonal symmetry. At high temperatures, the stability of the NaCl-type structure with fully occupied sublattices was accounted for by using an approach based on band energy smearing. The small carbon and oxygen admixtures do not stabilize the cubic phase compared to the hexagonal one. The stability of the cubic- and hexagonal-based phases was accounted for by drawing a parallel between the densities of states around the Fermi energy and phase stability: the lower the densities of states at the Fermi energy is, the lower the total energy is. The predicted structural transformations in stoichiometric vanadium nitrides are consistent with those observed experimentally.

ACKNOWLEDGMENTS

This work was supported by the National Academy of Science of Ukraine, Contracts No. III-15-09 and 71/11-H. The work of P. T. was performed under the auspices of the U. S. Department of Energy by the Lawrence Livermore National Laboratory under contract No. DE-AC52-07NA27344.

[1] L. E. Tot, *Transition Metal Carbides and Nitrides* (Academic, New York, 1971).

[2] O. N. Carlson, J. F. Smith, and R. H. Hafziger, Metall. Trans. A **17A**, 1647 (1986).

[3] V. A. Gubanov, A. L. Ivanovsky, and V. P. Zhukov, *Electron Structure of Refractory Carbides and Nitrides* (Cambridge University Press, Cambridge, 1994).

[4] F. Kubel, W. Lengauer, K. Yvon, K. Knorr, and A. Junod, Phys. Rev. B **38**, 12908 (1988).

[5] W. Weber, P. Rödhammer, L. Pintschovious, W. Reichardt, F. Compf, and A. N. Christensen, Phys. Rev. Lett. **43**, 868 (1979).

[6] E. I. Isaev, S. I. Simak, I. A. Abrikosov, R. Ahuja, Yu. Kh. Vekilov, M. I. Katsnelson, A. I. Lichtenstein, and B. Johansson, J. Appl. Phys. **101**, 123519 (2007).

[7] V. I. Ivashchenko and P. E. A. Turchi, Phys. Rev. B **78**, 224113 (2008).

[8] C. Ravi, CALPHAD **33**, 469 (2009).

[9] C. Ravi, H. K. Sahu, and M. C. Valsakumar, Phys. Rev. B **81**, 104111 (2010).

[10] D. L. Price and B. R. Cooper, Phys. Rev. B **39**, 4945 (1989).

[11] H. W. Hugosson, O. Eriksson, L. Nordstrom, U. Jansson, L. Fast, A. Delin, J. M. Wills, and B. Johansson, J. Appl. Phys. **86**, 7558 (1999).

[12] S. Baroni, A. Dal Corso, S. de Gironcoli, P. Giannozzi, C. Cavazzoni, G. Ballabio, S. Scandolo, G. Chiarotti, P. Focher, A. Pasquarello, K. Laasonen, A. Trave, R. Car, N. Marzari, and A. Kokalj, (2011), `http://www.pwscf.org/`.

[13] D. Vanderbilt, Phys. Rev. B **41**, 7892 (1990).

[14] J. P. Perdew, K. Burke, and M. Ernzerhof, Phys. Rev. Lett. **77**, 3865 (1996).

[15] H. J. Monkhorst and J. D. Pack, Phys. Rev. B **13**, 5188 (1976).

[16] S. R. Billeter, A. Curioni, and W. Andreoni, Comput. Mater. Sci. **27**, 437 (2003).

[17] S. Baroni, S. De Gironcoli, A. Dal Corso, and P. Gianozzii, Rev. Mod. Phys. **73**, 515 (2001).

[18] V. I. Ivashchenko, P. E. A. Turchi, and E. I. Olifan, Phys. Rev. B **82**, 054109 (2010).

[19] D. A. Papaconstantopoulos, W. E. Pickett, B. M. Klein, and L. L. Boyer, Phys. Rev. B **31**, 752 (1985).

[20] C. Wang, W. Wen, Y. D. Su, L. Xu, C. Q. Qu, Y. J. Zhang, L. Qiao, S. S. Yu, W. T. Zheng, and Q. Jiang, Solid State Commun. **149**, 725 (2009).